Journal of Molecular Graphics and Modelling 51 (2014) 104–112

Contents lists available at ScienceDirect

Journal of Molecular Graphics and Modelling

journal homepage: www.elsevier.com/locate/JMGM

Identification of a high affinity selective inhibitor of Polo-like kinase 1 for cancer chemotherapy by computational approach

Manoj Kumar[a], Sai Prasad Pydi[a,b], Sujata Sharma[a], Tej P. Singh[a], Punit Kaur[a,*]

[a] Department of Biophysics, All India Institute of Medical Sciences, New Delhi 110 029, India
[b] Department of Oral Biology, University of Manitoba, Winnipeg, Manitoba, Canada R3T 2N2

ARTICLE INFO

Article history:
Accepted 28 April 2014
Available online 6 May 2014

Keywords:
Anti-cancer drugs
Polo-like kinase
Structure-based drug design
Homology modelling
Molecular docking
Molecular dynamics simulation

ABSTRACT

Polo-like kinase (Plk)1 is a key regulator of the cell cycle during mitotic phase and is an attractive anti-mitotic drug target for cancer. Plk1 is a member of Ser/Thr kinase family which also includes Plk2-4 in human. Plk1 promotes the cell division whereas Plk2 and Plk3 are reported to act as tumour suppressors. The available inhibitors of Plk1 also suppress Plk2 and Plk3 activity significantly resulting in the cell death of normal cells in addition to the cancer cells. Hence, it is imperative to explore Plk1 specific inhibitors as anti-cancer drugs. In this work, a selective potential inhibitor of Plk1 has been identified by molecular docking based high throughput virtual screening. The identified compound exploits the subtle differences between the binding sites of Plk1 and other Ser/Thr kinases including Plk2-4. The predicted binding affinity of identified inhibitor is higher than available inhibitors with a 100-fold selectivity towards Plk1 over Plk2-4 and several cell cycle kinases. It also satisfies the Lipinski's criteria of drug-like molecules and passes the other ADMET filters. This triazole compound with aryl substituent belongs to a novel class of potential inhibitor for Plk1. The suggested potential lead molecule can thus be tested and developed further as a potent and selective anti-cancer drug.

1. Introduction

The regulatory proteins like cyclin-dependent kinases and Ser/Thr kinases in the cell cycle have recently been targeted for determining alternative suitable anti-cancer drug candidates with low levels of cytotoxicity. Amongst the Ser/Thr kinases, Polo-like kinase (Plk)1 has gained importance as an attractive anti-cancer drug target [1]. Plk1 is highly expressed in proliferating cells and has been seen to be overexpressed in 80% of human tumours and cancer cells of diverse origins including colorectal and lung carcinoma, glioma, melanoma, head and neck cancer, ovarian cancer and breast cancer [2,3]. Its overexpression has also been correlated with poor prognosis in a broad spectrum of malignancies [4,5]. The antisense oligonucleotides (siRNA) targeting the mRNA of Plk1 have been shown to reduce cell proliferation in several cancer cell lines and exhibit no visible effect on the viability of untransformed cells [6,7]. The inhibition of enzymatic activity of Plk1 is known to arrest the tumour cells in mitosis subsequently leading to apoptosis [8]. Hence, Plk1 serves as an important target for the development of anti-cancer drugs.

Till date, five members of human Plks have been reported: Plk1, Plk2/Snk, Plk3/Fnk/Prk, Plk4/Sak and Plk5. The Plk family is highly conserved from yeast to mammals and are structurally similar, yet, they exhibit significant differences in their cellular functions [9]. Out of these five Plks, the biological roles of Plk1, Plk2 and Plk3 have been extensively studied. Plk1 regulates the cell cycle during late G2 and M phases while Plk2 and Plk3 regulate the cell cycle during G1 and S phases. Plk1 is involved in activation of cyclin-dependent kinase, checkpoint kinase, mitotic entry, chromosome alignment, centrosome maturation, bipolar spindle formation, activation of anaphase promoting complex, chromatid separation, mitotic exit and initiation of cytokinesis [10–13]. Plk2 and Plk3 act as tumour suppressor. Plk2 is believed to be involved in DNA damage checkpoints [14] while Plk3 is required for the entry into S-phase [15,16]. Plk4 is less conserved compared to Plk1-3 and functionally it is involved in the duplication of centriole in the cell cycle [17]. Plk5 has recently been reported and unlike human Plk1-4, it does not play a role in the cell cycle [18]. Hence, a potent inhibitor of Plk1 that does not inhibit the enzymatic activity of other Plks or inhibits them with low potency as compared to Plk1 can act as an ideal anti-cancer drug candidate.

Structurally, the Plks are characterized by one or more polo box domain (PBD) at C-terminus and a catalytic domain of Ser/Thr kinase at N-terminus. In addition to the kinase domain, Plk1-3 each

* Corresponding author. Tel.: +91 11 2658 4288; fax: +91 11 2658 8663.
E-mail addresses: punitkaur1@hotmail.com, punit@aiims.ac.in (P. Kaur).

http://dx.doi.org/10.1016/j.jmgm.2014.04.014
1093-3263/

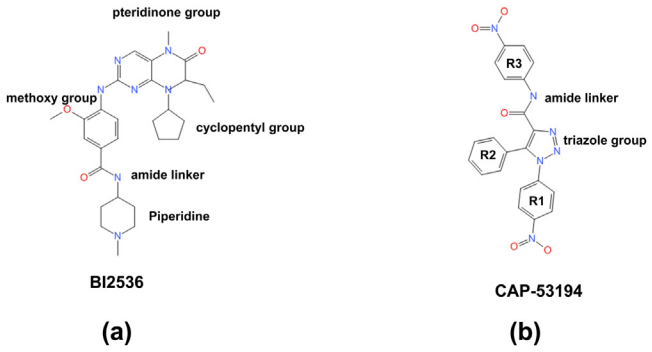

Fig. 1. Chemical structure of (a) known potent inhibitor BI2536 and (b) potential inhibitor CAP-53194 identified by virtual screening.

contain two PBDs whereas Plk4 possesses only one PBD. Plk5 is distinct as it contains one PBD and lacks the kinase domain. The PBD possesses regulatory activity and is responsible for the proper localization of Plks to their targets [19]. The catalytic domain of Ser/Thr kinase possesses an ATP binding pocket. Majority of the reported inhibitors till date developed against this catalytic domain are either ATP analogues or non-ATP small molecule inhibitors that target the ATP binding pocket [1]. The ATP binding site is highly conserved amongst all the Ser/Thr kinases including the four Plks. This makes the design and identification of Plk1 specific inhibitors a challenging task. Currently reported inhibitors of Plk1, to our knowledge, are not specific or sufficiently selective over other important cellular Ser/Thr kinases and produce side effects due to their cytotoxic effects on normal cells. Wortmannin, an ATP competitive inhibitor of Phosphatidylinositol 3-kinase (PI3K), inhibits Plk1 with an inhibition constant of 24 nM but is known to covalently modify the protein leading to toxicity [20]. Scytonemin, a natural product isolated from cyanobacteria, blocks Plk1 with a potency of 2 μM [21] but simultaneously suppresses cyclin dependent kinase, checkpoint kinase 1 and protein kinase C with nearly similar potency. Thiophene benzimidazole derivative is a novel class of Plk inhibitor which targets the ATP binding pocket of Plk1 but is also reported to inhibit Plk3 with similar potency [22]. ZK-Thiazolidinone, a non-competitive ATP inhibitor, possessing IC_{50} value of 19 nM for Plk1 has concurrently an IC_{50} value of approximately 100 nM for Plk2 and Plk3 [23]. High throughput screening followed by lead optimization has identified an ATP-competitive dihydropteridinone derivative based potent inhibitor of Plk1, BI2536 (Fig. 1a) [24]. This is reportedly one of the best known inhibitor of Plk1 in terms of its activity and selectivity (IC_{50} = 8 nM) with up to 50-fold selectivity over other Ser/Thr kinases. It, however, also prevents Plk2 and Plk3 activity to a similar extent [25]. Thus, the currently known inhibitors of Plk1 simultaneously inhibit Plk2 and Plk3 equally resulting in cytotoxicity. Hence, potent inhibitors of Plk1 selective over Plk2 and Plk3 and other cellular Ser/Thr kinases could provide a suitable lead molecule for the development of less toxic anti-cancer drugs.

This prompted us to explore the possibility of identifying a lead molecule based on sequence and structural information. The sequence analysis of the kinase domain of Plks revealed differences in the nature of residues between Ser/Thr kinase domain of Plk1 and other kinases including Plk2-4. The residues Leu132, Arg134 and Arg136 in the ATP binding pocket are relatively specific to Plk1. The corresponding residues in other kinases are generally Tyr/Phe, Ser/His and Gly, respectively. The selectivity determining methoxy group of ligand BI2536 occupies the small cavity provided by Leu132 in Plk1 [25]. This residue in Plk2 is replaced by the bulkier Tyr residue which reduces the binding space for BI2536 and results in steric hindrance to its methoxy group. Moreover, Plk1 has a large and positively charged residue Arg134 while the corresponding residue in Plk2 and Plk3 is relatively a smaller and neutral serine. In the present study, we have exploited these subtle differences in the key residues at the active site of Plks and other kinases to identify a potentially more selective inhibitor of Plk1 using the combined approach of molecular docking and virtual screening of chemical database.

2. Materials and methods

The X-ray crystal structures of several Plk1-ligand complexes are available. The structure with the highest resolution amongst the available crystal structure of human Plk1 complexed with inhibitors at 1.9 Å resolution with the highly potent inhibitor BI2536 (PDB: 2RKU) was chosen for this study [25,26]. This was used as receptor for identification of high affinity inhibitors of Plk1 during structure-based virtual screening of chemical library. Three-dimensional (3-D) structures of Plk2-4 were also crucial for the structure-based study as the potential inhibitors identified by virtual screening were screened for their selectivity against them. Since the structures of Plk2 and Plk3 are not available, these were homology modelled using the crystal structure of Plk1 as their Ser/Thr kinase domain shares more than 50% sequence homology with Plk1. The available crystal structure of Plk4–ATP analogue complex (PDB: 3COK) was used for selectivity study. Plk5 was excluded from this study as it lacks the kinase domain and is characterized by only the PBD domain. All the computational analyses has been carried out in the modelling environment of Discovery Studio (DS) 2.0 [27] using CHARMm 33.1 [28,29] force field and LigandFit [30] docking protocols.

2.1. Homology modelling of Plk2 and Plk3

The residues located at the ATP binding pocket in human Plk1 are more conserved in Plk2 and Plk3 than Plk4. The catalytic domains of Plk2 and Plk3 share a sequence identity of 52.6% (similarity 77.1%) and 53.0% (similarity 76.3%), respectively with Plk1. In the absence of crystal structures of Plk2 and Plk3 catalytic domains, their model structures were generated by homology modelling using Plk1 as template with the help of MODELLER 9v3 [31,32]. Ten homology models each for both Plk2 and Plk3 were generated and the best two models, one for each protein, were selected based on the Probability Density Function (PDF) energy [31] and Discrete Optimized Protein Energy (DOPE) score [33]. PDF energy is the sum of all the homology derived and stereochemical pseudo-energy terms while DOPE score is the atomic based statistical potential which is a measure of the stability of a conformation. As a lower value for both PDF Energy and DOPE score is indicative of a better model, the model with lowest PDF energy as well as DOPE score amongst the 10 generated models obtained for each protein (Plk2 and Plk3) was selected for further analysis. The stereochemical quality of the selected homology models was verified by PROCHECK [34]. The side chains of the selected models were refined using CHARMm force field 33.1 and conjugate gradient algorithm with convergence criteria of root mean square (r.m.s.) gradient less than 0.05 kcal mol^{-1} $Å^{-1}$. The two minimized models for Plk2 and Plk3 were further refined by short molecular dynamics (MD) simulations of 200 ps of equilibration followed by 200 ps of production run in the presence of water solvent model (TIP3P) to relax their model structures.

2.2. Receptor preparation

The binding site residues are nearly conserved amongst the four human Plks except in Plk4 where they are comparatively less conserved. Therefore, it was imperative to dock and cross

check and evaluate the interactions of the ligand and its respective affinity for different Plks. To obtain a correct and meaningful docking analysis, it is first necessary to prepare and process the protein structures. As an initial step, the crystallographic water molecules and ligand were removed from the co-crystal structure of Plk1–BI2536 (PDB: 2RKU) [25]. Subsequently, the protein and its geometry was cleaned *i.e.* connectivity and bond orders were corrected, alternate conformations were removed retaining one set of side chain conformation. The force field parameters of all atom CHARMm 33.1 were assigned and partial charges added. The hydrogen atoms were included and their positions optimized keeping the protein backbone rigid by Adopted Basis set Newton Raphson (ABNR) minimization algorithm in the presence of the distance dependent dielectric solvent model with the convergence criteria of r.m.s. gradient less than 0.05 kcal mol^{-1} $Å^{-1}$. The binding site for docking studies was defined in the ATP binding pocket around the ligand BI2536. A sphere with a radius of 5 Å from the centre of the binding site was defined and the side chains of the residues within this sphere were treated as flexible during the refinement of the docked poses. The minimized protein with the defined binding site was taken as the receptor for docking study with BI2536 and the various compounds of the chemical library during molecular docking based virtual screening.

The refined homology model structures of Plk2 and Plk3 were also used as receptor models for molecular docking. The binding sites for docking studies were defined in a manner similar to Plk1. The receptor for docking analysis in the case of Plk4 was prepared using its crystal structure (PDB Id: 3COK). These prepared receptors were initially used for docking BI2536 for verification of docking protocol and subsequently potential hits obtained for Plk1 from virtual screening experiments to determine their relative binding strength for Plk1 over Plk2-4.

2.3. Docking and scoring

Molecular docking is a computational method to estimate the correct fit of two molecules in terms of shape and interactions. This method can be used to predict the most probable binding mode of the ligand in the binding site of receptor by varying the ligand position and conformation. LigandFit [30] docking protocol has been used for the docking studies of ligands with the Plks. This docking algorithm combines a shape comparison filter with a Monte Carlo conformational search to generate docked poses consistent with the binding site shape of the rigid receptor. The initial poses obtained were refined by rigid body minimization of the ligand with respect to the calculated grid-based interaction energy using the Dreiding force field [35] and the docked poses were ranked according to Dock score. The final minimization of the rigid body minimized docked poses was performed with full potential minimization. This was carried out in the presence of flexible side chains of the proteins within 5 Å of the binding site using all-atom CHARMm force field 33.1 and conjugate gradient minimization method with a convergence criteria of less than 0.05 kcal mol^{-1} $Å^{-1}$ r.m.s. gradient. The refined poses were re-scored by eleven scoring functions available in DS 2.0. The aim was to identify the most probable binding conformation of the ligand and determine the suitable scoring function which gave the best docked pose.

2.4. Validation of docking and scoring method

The docking accuracy and scoring method was first assessed for its ability to predict the bound conformation and binding affinity with the experimental value of the known inhibitor. The bond order of ligand BI2536 (Fig. 1a) was corrected after extracting it from co-crystal complex of Plk1 (PDB Id: 2RKU) [25] by converting the partial double bond in the phenyl ring of BI2536 into alternating single double bonds to enable the assignment of suitable force field parameters to the compound. Subsequently, MMFF 94 force field parameters were assigned and partial charges added. The hydrogen atoms were generated and their positions optimized adopting the methodology similar to the receptor. The optimized ligand was docked back into the binding site using LigandFit docking protocol and analysed for its docked conformation with respect to the crystal structure. The docked poses were also scored employing empirical scoring functions that estimate their K_d values. The advantage of using empirical scoring function is that it can also estimate the binding strength (K_d) of the docked ligand in addition to the ranking of the binding mode of docked poses. The calculated K_d of BI2536 obtained by each empirical scoring function was compared with its experimentally determined binding constant. Similarly, BI2536 was docked into the prepared receptor proteins of Plk2-4 and analysed following the strategy adopted for Plk1.

2.5. Virtual screening and selectivity study

Virtual screening of ligands was carried out with the chemical library of small molecules, LigandFitCAP2002 [36]. This contains the two-dimensional structures of 141,639 ligands from database of Chemicals Available for Purchase (CAP). These ligands were subjected to 'Prepare Ligands' protocol which ionizes the ligands in the pH range of 7 to 8, generates the tautomers, enumerates stereomers (if any), applies Lipinski's filter [37,38] and generates their three-dimensional (3-D) conformations using the program Corina [39,40]. The Lipinski's rule of 5 was used to filter the oral-bioavailable drug-like molecules based on the criteria of molecular weight less than 500 Da, number of hydrogen bond donor ≤ 5 and acceptor ≤ 10 and log P value lesser than 5. The prepared compounds obtained from the initial screening with drug-like properties consisted of 39,300 different molecules. The filtered and prepared library of chemical compounds was subsequently screened for the Plk1–ATP binding pocket to find potential inhibitors using docking protocol of LigandFit. The prepared receptors of Plk2-4 were subsequently docked with the top ranked potential inhibitor identified by virtual screening to estimate the relative binding strength and examine the interaction pattern of this compound with the different proteins of Plk family.

2.6. Molecular dynamics simulations

The molecular dynamics (MD) simulation was initially performed on the docked complex of Plk1 with the best potential inhibitor in the presence of water solvents to study their binding stability using CHARMm simulation engine in the modelling environment of DS 2.0. As the receptor was kept rigid during the docking process, the docked complex was energy minimized by conjugate gradient algorithm with convergence criteria of r.m.s. gradient of 0.05 kcal mol^{-1} $Å^{-1}$ to remove van der Waals clashes and relax the complex. The minimized complex was solvated with TIP3P solvent model [41] with spherical boundary condition in the presence of harmonic restraint and minimized in three steps employing decreasing order of simulation constraints. The solvent molecules of hydrated protein-ligand complex were minimized during the first step using Steepest Descent algorithm with convergence criteria of r.m.s. gradient less than 0.1 kcal mol^{-1} $Å^{-1}$ in the presence of rigid protein. The second step involved minimization of this solvated complex using Conjugate Gradient algorithm with convergence criteria of r. m. s gradient less than 0.05 kcal mol^{-1} $Å^{-1}$ keeping the backbone of the protein rigid. In the third step of minimization, the Adopted Basis-set Newton–Raphson (ABNR) algorithm was applied with convergence criteria of less than 0.01 kcal mol^{-1} $Å^{-1}$ r.m.s. gradient without any constraints. The simulation was also performed in three stages consisting of

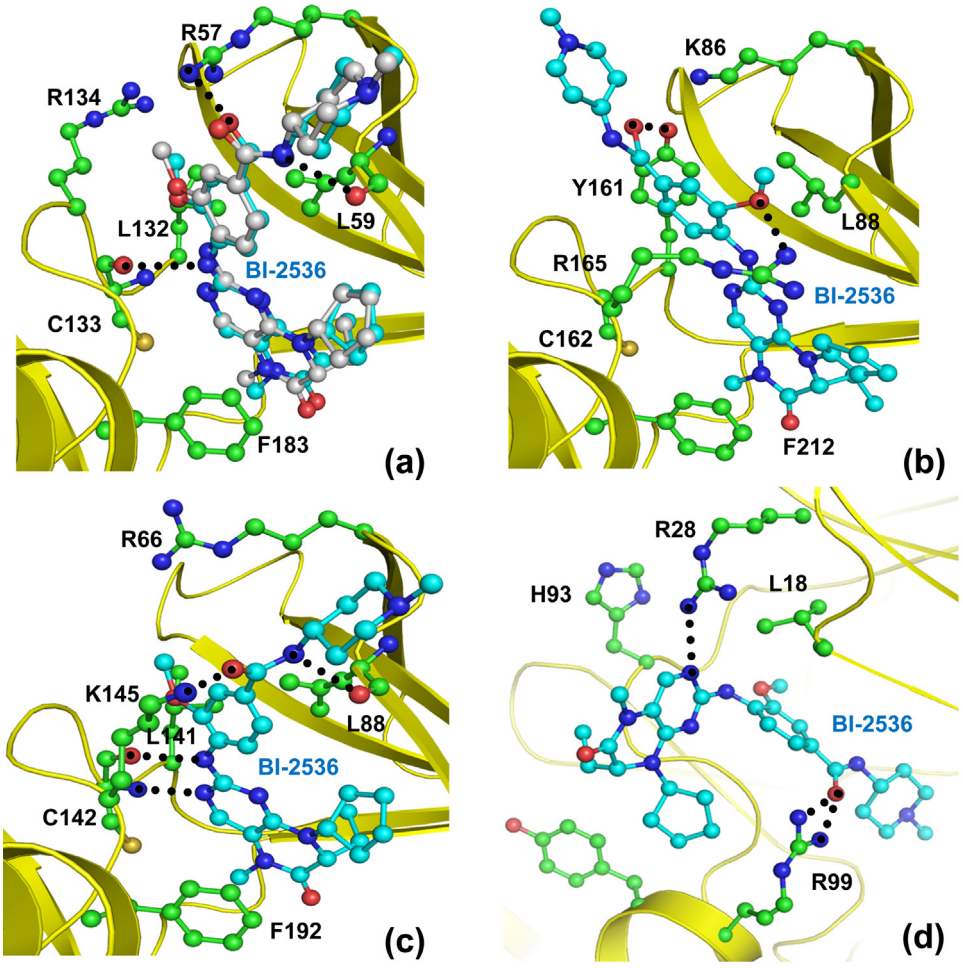

Fig. 2. Docked conformation of BI2536 (cyan) (a) superimposed on the conformation in the crystal structure of Plk1 (b) in Plk2 (c) in Plk3 and (d) in Plk4. Hydrogen bonds between docked conformation and selected binding site residues of respective Plks are shown as black dotted lines. All figures were produced using PyMol v0.99 [45].

sequential heating, equilibration and production runs. In the first stage, the temperature of the system (minimized hydrated complex) was raised from 50 K to 300 K in the presence of rigid backbone of the protein. Next, the system was equilibrated for 2 ns at the target temperature of 300 K with the help of 'adjust velocity frequency' method. In both the heating and equilibration stages of simulation, the frequency of velocity adjustment was 50. The final stage of simulation comprised a production run for NVT (constant temperature dynamics) ensembles carried out for 10 ns using Leapfrog Verlet dynamics integrator in the presence of 'Berendsen coupling bath' [42] taking a temperature coupling decay time of 5 ps. A time step of 1 fs was utilized in all the three stages of simulation.

2.7. ADMET studies

All the compounds obtained by virtual screening are not ideal candidates as lead molecules to be developed further as drugs. Thus it is imperative to initially filter out the hit molecules which have the physico-chemical properties for becoming probable drug candidates. The pharmacokinetic and pharmacodynamic properties play a significant role in the drug design process as they account for a large number of drug failures occurring in clinical trials. These properties were analysed using the ADMET (Absorption, Distribution, Metabolism, Excretion and Toxicity) descriptor. The ADMET involves the calculation of the molecular properties and relating them to the experimentally determined pharmacokinetic profiles. The retrieved molecules from the database were assessed *in silico* for these properties by employing the ADMET descriptors and TOPKAT protocol available in DS 2.0.

3. Results and discussion

3.1. BI2536 and Plk1: docking protocol validation

The optimization and validation of the docking protocol and scoring functions with the experimental values is essential for the screening accuracy. The docking protocol in this study was validated by comparing the docked position and conformation of BI2536 with respect to its crystal structure. A total of 11 different scoring functions (LigScore1, LigScore2, Jain Score, PMF (Potential of Mean Force), PMF04, PLP (Piecewise Linear Potential) 1, PLP2, Ludi1, Ludi2, Ludi3 and Dock Score) were used to assess their predictive power to reproduce the crystal geometry for BI2536 in the ATP binding pocket of Plk1. The conformation obtained using Ludi3 score [43] out of 11 scoring functions was found to be closest to the crystal geometry of BI2536. The superimposition of BI2536 indicated that the docked and crystal conformations overlapped well with a positional r.m.s. deviation of 0.5 Å (Fig. 2a) which is within the permissible error range as a value of below 2 Å is considered to be successful docking [44]. This suggested the suitability of LigandFit docking protocol in combination with Ludi3 scoring function to reproduce the correct geometry of the reported inhibitor BI2536. Ludi3 is an empirical scoring function which also

Table 1
Corresponding residues of binding site in Plks with the respective numbering scheme in brackets.

Residues position in Plk1	Plk1	Plk2	Plk3	Plk4
57	R	K (86)	R (66)	N (16)
58	F	V (87)	L (67)	L (17)
59	L	L (88)	L (68)	L (18)
61	K	K (90)	K (70)	K (20)
67	C	C (96)	C (76)	V (26)
69	E	E (98)	E (78)	R (28)
80	A	A (109)	A (89)	A (39)
114	V	V (143)	V (123)	L (73)
130	L	L (159)	L (139)	L (89)
131	E	E (160)	E (140)	E (90)
132	L	Y (161)	L (141)	M (91)
133	C	C (162)	C (142)	C (92)
134	R	S (163)	S (143)	H (93)
136	R	R (165)	K (145)	G (95)
140	E	H (169)	H (149)	R (99)
183	F	F (212)	F (192)	L (142)

calculates the binding strength (K_d) of docked ligands besides the ranking of docked poses. It estimates the free energy of binding of protein-ligand complex with known 3-D structure based on hydrogen bond interactions, ionic interactions, lipophilic interactions, number of rotatable bonds in the ligand. It is calculated as Ludi3 score = $-100 \log K_d$ and $\log K_d = -\Delta G/2.303$ RT and has a standard error of 1.75 kcal mol^{-1}. The corresponding error in the estimated binding affinity using Ludi3 scoring function can vary up to 20 times the experimental value of binding affinity [43]. The calculated K_d value (21.4 nM) of BI2536 for Plk1 was about 2-fold different than the experimentally determined IC_{50} value (8.0 ± 2.9 nM) [25] and was within the limit of accuracy. Hence, this docking protocol and scoring function was used to identify the potential hits during virtual screening.

3.2. Plk2-4: comparison of molecular docking of BI2536

The binding site of Ser/Thr kinase domain in Plk1-4 though structurally conserved exhibits significant sequence variations. The details of the residues in Plk1 and the corresponding residues in other Plks with the numbering scheme are provided in Table 1. The docking protocol was validated for Plk2-4 employing the same strategy as Plk1 where Ludi3 with LigandFit emerged as the protocol of choice. BI2536 docked into the binding pocket of Plk2-3 wherein its pteridinone moiety occupied a position similar to Plk1 and interacted with the corresponding Phe residue (Phe183 of Plk1) through π–π aromatic interactions (Fig. 2a-d). In contrast the conformation adopted in Plk4 was different due to the presence of Leu instead of the corresponding Phe residue.

In Plk2, BI2536 was observed to adopt a different orientation in the binding pocket. This may be attributed to the replacement of residue Leu132 in Plk1 by Tyr161 in Plk2. The bulky aromatic ring of Tyr161 in Plk2 narrows down the available space in the cavity leading to the inability of the proper placement of the methoxy group of BI2536 which is forced to move in an opposite direction (Fig. 2b). The position occupied by the pteridinone moiety remains similar to Plk1 and Plk3 and it interacts through π–π aromatic interactions with Phe212. Furthermore, the binding of BI2536 with Plk2 is further stabilized by three unique interactions not observed in Plk1: (i) hydrogen bonded interaction between oxygen atom of methoxy group and side chain of Arg165, (ii) hydrogen bond formation between oxygen atom of amide linker and hydroxyl group of Tyr161 and (iii) π–π aromatic interactions between the phenyl rings of ligand and Tyr161.

The docked conformation of BI2536 in Plk3 is observed to be almost identical to Plk1 (Fig. 2a and c) and has the same order of calculated binding affinity and interaction energy. A number of commonalities were observed between the docked conformations in the two proteins. The selectivity determining methoxy group of BI2536 occupies the small sub-pocket created by residue Leu132. The nitrogen atom of amide linker as well as amino group of pteridinone moiety forms hydrogen bonded interactions with carboxyl atoms of Leu88 and Cys142, respectively. The difference in affinity of BI2536 to Plk1 and Plk3 can be attributed to the differential binding of the amide linker oxygen atom which is hydrogen bonded with Arg57 in Plk1 but Lys145 in Plk3. The calculated K_d of BI2536 for Plk3 (28.8 nM) was in the vicinity of the experimentally determined value (IC_{50} = 13.6 ± 7.3 nM) [25]. The lower affinity of the ligand for Plk3 may be due to weaker van der Waals interactions owing to the presence of Ser instead of Arg134 as observed in Plk1.

A sequence comparison indicates that the binding site residues in Plk4 are less conserved amongst human Plks. The residues Leu132, Arg136, Glu140 and Phe183 in Plk1 are replaced by Met91, Gly95, Arg99 and Leu142, respectively in Plk4. This leads to a conformational rearrangement of amino acid residues at the binding site region resulting in an alteration in its shape and nature. Another crucial residue, Phe183 in Plk1, is substituted by Leu142 in Plk4 resulting in its inability to stabilize the aromatic pteridinone moiety of BI2536 through π–π interactions. These significant alterations in the binding site region result in the turnaround of the orientation of BI2536 in Plk4 in contrast to Plk1-3 (Fig. 2d). The pteridinone moiety along with cyclopentyl group is seen to move closer towards the protein surface. The docked ligand is stabilized by hydrogen bonds formed between nitrogen atom of pteridinone moiety and residue Arg28 and oxygen atom of amide linker and residue Arg99.

3.3. Virtual screening of LigandFitCAP2002 library

The initial screening of LigandFitCAP2002 database (141,300 compounds) on the basis of Lipinski's filter reduced the number of compounds for further analysis to 39,300 ligands. *In silico* screening of these ligands from prepared library was performed with Plk1 using LigandFit docking protocol and Ludi3 scoring function. All these compounds were then docked into the binding site of Plk1. 25,513 compounds failed to dock due to lack of size and shape complementarities with the binding site. From the 13,787 successful docked molecules, 138 compounds were further filtered out which had binding affinity of less than or equal to 1 μM based on Ludi 3 score. Filtering criteria of binding affinity was further raised by 5-fold *i.e.* 200 nM from 1 μM to ensure elimination of low affinity potential hits and enable selection of probable higher affinity hits. 20 top hits so obtained with predicted binding affinity of approximately 200 nM were taken up for detailed analysis of their docked conformations and interactions. These 20 hits were examined for unfavourable conformational energy of the docked ligand and 5 hits with positive internal energy in the docked conformation were discarded. 6 hits of the surviving 15 hits, with a calculated binding affinity (K_d) of 100 nM or higher were subsequently further evaluated. The docked complex of these 6 hits was energy minimized to remove any avoidable short contacts since the receptor protein was kept rigid during docking process. These energy minimized docked complexes were manually analysed qualitatively and quantitatively for interactions with receptor and their interaction energy calculated using CHARMm 33.1 force field parameters in the presence of distance dependent dielectric implicit solvent model. The hits possessing both a higher K_d and negative interaction energy were finally chosen. Two such hits were found to have calculated K_d higher than 5 nM. The two hits have identifier/CAP key of 14442 (CAP-14442) and 53194 (CAP-53194). CAP-14442 has a calculated binding affinity of 4.8 nM and CAP-53194 of 0.6 nM. Since CAP-53194 displayed better binding affinity and interaction energy this molecule was taken up for further analysis. CAP-53194

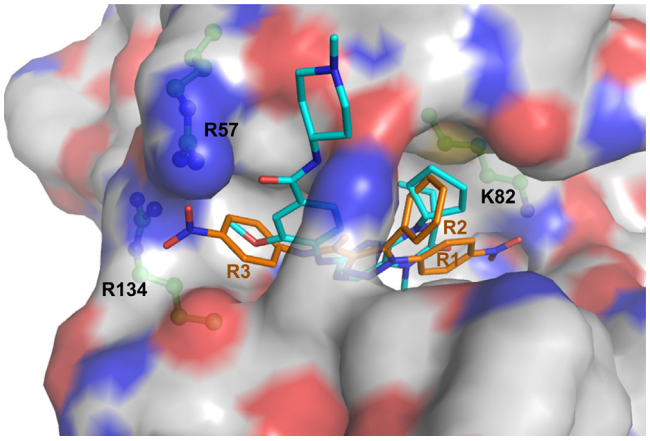

Fig. 3. Superimposition of docked conformation of the identified compound CAP-53194 (orange, ball-and-stick) on docked BI2536 (cyan, ball-and-stick) showing side chain of selected residues of Plk1 (green, ball and stick). (For interpretation of the references to colour in this figure legend, the reader is referred to the web version of the article.)

contains two nitrophenyl moieties (R1 and R3), one phenyl ring (R2), one triazole ring and an amide linker linking triazole ring with R3 nitrophenyl moiety (Fig. 1b).

3.4. Binding of CAP-53194 with Plk1

The best hit identified in terms of calculated K_d and interaction energy from the LigandFitCAP2002 library through structure based virtual screening was CAP-53194. Thus this compound was taken up for further analysis of its specificity and binding properties with the four Plk proteins. CAP-53194 docked in the ATP binding pocket of Plk1 and adopted an orientation similar to BI2536 (Fig. 3). The position of triazole ring and nitrophenyl ring (R1) partially overlap the pteridinone moiety of BI2536. The phenyl ring (R2) and nitrophenyl moiety (R3) of CAP-53194 coincides with cyclopentyl ring and methoxy group of BI2536, respectively. Its phenyl ring of the R1 moiety like pteridinone moiety of BI2536 is stabilized by π–π aromatic interactions with the phenyl ring of Phe183, R2 phenyl ring is stabilized by cation–π interactions with guanidinium group of Arg136 whereas the phenyl ring of R3 moiety is sandwiched between Leu59 and alkyl chain of Arg134 side chain. This identified compound, however, enters deeper into the binding cavity than BI2536 and its R1 nitro group is engaged in the formation of hydrogen bonded interactions with Lys82 Nz atom and main chain nitrogen atom of Asp194 (Fig. 4a). BI2536 piperidine moiety is seen to overhang outside whereas the R3 moiety of CAP-53194 remains inside the binding pocket with its nitro group forming hydrogen bonded contacts with guanidinium groups of Arg57 and Arg134. The oxygen atom of amide linker is observed to be hydrogen bonded with Arg136 NH2 while its nitrogen atom forms hydrogen bond with carboxyl atom of Cys133. Like BI2536, hydrogen bonded interactions involving Cys133 and Arg57 as well as π–π interactions with Phe183 are also observed in CAP-53194. The hydrogen bonded interactions between nitro group and triazole moiety of compound CAP-53194 with binding site residues of Plk1 leads to an increase in its binding strength. The predicted binding affinity (K_d) of compound CAP-53194 for Plk1 of 0.62 nM is about 13-fold higher than that for BI2536. The larger number of strong interactions with Plk1 and lower total interaction energy of −78.56 kcal mol^{-1} when compared to BI2536 (−68.30 kcal mol^{-1}) supports that this new ligand possesses higher affinity for Plk1 than known inhibitor BI2536.

3.5. Binding of CAP-53194 with Plk2-4: a selectivity study

The selectivity of a drug constitutes a major problem in drug discovery. For a designed compound to be a successful drug candidate, it is essential that it can discriminate between the desired target and other macromolecular targets which possess similar structures. The identified candidate drug is an ATP-site binder and the Plk protein family and other kinase proteins share a marked homology at the ATP-binding site. The ATP pocket harbours a number of conserved residues which impart it specificity for interacting with its binders. Notwithstanding, these conserved residues, a careful scrutiny of the ATP-binding region indicated that there exist explicit residues which fine tune these sites and permit discriminately differential binding of the candidate drug molecule to these different protein molecules. Hence, it was imperative to investigate the binding affinity of CAP-53194 with other Plks in relation to Plk1.

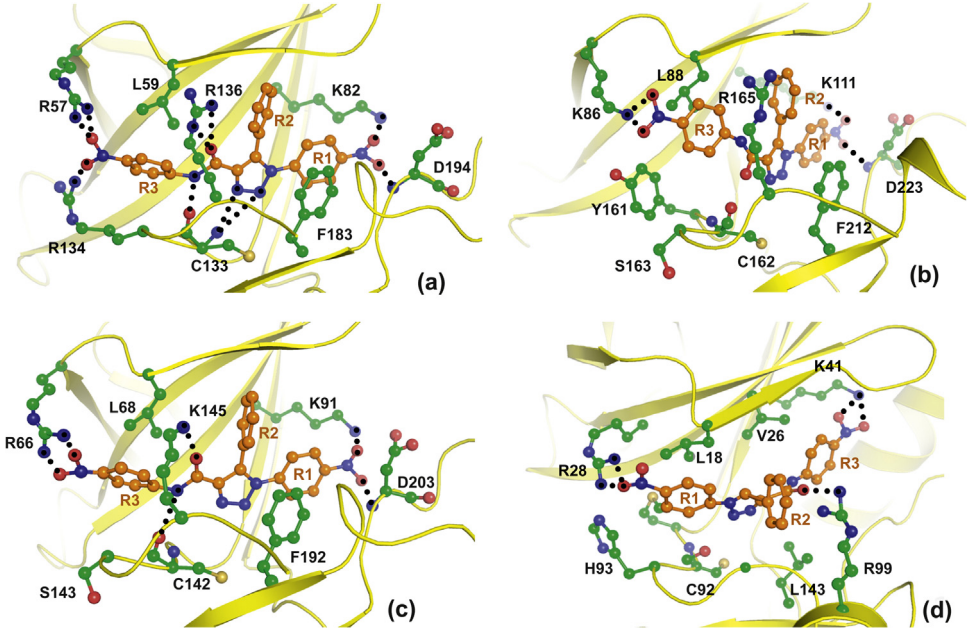

Fig. 4. Potential inhibitor CAP-53194 (orange, ball-and-stick) docked in (a) Plk1, (b) Plk2, (c) Plk3 and (d) Plk4. The colouring and rendering correspond to Fig. 2.

Table 2
Selectivity of CAP-53194 against protein kinases involved in cell cycle.

Kinases	Predicted binding affinity (K_d) for CAP53194 (nM)	Selectivity index for Plk1
Plk1	0.62	–
Plk2	72.4	117
Plk3	44.7	72
Plk4	119.3	192
CDK2	323.6	522
CHK1	457.1	737
AuroraA	549.5	872
PKA	398.0	641
AKT1	246.5	398
EGFR	288.4	458
ABL	234.4	378
NEK2	269.1	434
cMET	371.5	599

The selectivity analysis of compound CAP-53194 for Plk1 over Plk2-4 was carried out by docking it with Plk2-4. The docking results indicate that the triazole moiety, R1 and R2 rings of CAP-53194 occupy a position in Plk2 and Plk3 similar to Plk1 while it is different in Plk4 as BI2536 (Fig. 4). Like Plk1, the hydrogen bonded pattern observed between nitro group on R1 ring of CAP-53194 and Lys82 as well as Asp194 is maintained with corresponding residues of Plk2 and Plk3. However, the hydrogen bond mediated interaction observed between CAP-53194 triazole moiety and Cys133 of Plk1 was absent in case of Plk2-4. Additional differences observed in interactions between Plk1 and Plk2-4 with CAP-53194 pointed to its selectivity for Plk1 over Plk2-4.

The further comparative analysis of docked position of CAP-53194 with Plk1 and Plk2 indicated significant differences in their interactions which can be attributed to alterations in the nature of residues at the binding pocket. In contrast to Plk1, the bulky Tyr161 in Plk2, forces the R3 moiety of CAP-53194 to move away with a rotation of about 90° along the amide linker resulting in the loss of three hydrogen bonded interactions with Cys162 and Arg165 (Fig. 4b). Similarly, the shorter Ser163 in Plk2 (Arg134 in Plk1) is incapable of interacting with nitro group on R3 moiety. This variation also results in the weakening of electrostatic attraction observed in Plk1 between negatively charged nitro group and positively charged guanidinium groups of Arg57 and Arg134. Overall, the loss of these important interactions reduce the binding affinity of CAP-53194 for Plk2 by more than 100-fold (Table 2). This is also supported by the calculated electrostatic interaction energy for Plk2 (-18.71 kcal mol^{-1}) in comparison to Plk1 (-41.58 kcal mol^{-1}).

The binding site residues between Plk1 and Plk3 are most conserved amongst human Plks. This is reflected in the observed conformation of compound CAP-53194 in the two structures. The hydrogen bond mediated interactions of amide linker and nitro group on R1 moiety were observed in both Plk1 and Plk3 (Fig. 4c). However, two significant modifications, Ser143 and Lys145 in Plk3 instead of Arg134 and Arg136 in Plk1 impart differential specificity. These alterations cause elimination of one hydrogen bond with nitro group of R3, reduction of its electrostatic attraction and weakening of cation–π interaction with R2 aromatic ring as compared to Plk1 resulting in 70-fold reduction in binding affinity of CAP-53194 for Plk3 (Table 2). This is supported by the loss of calculated electrostatic interaction energy (-28.47 kcal mol^{-1}) for Plk3 as compared to Plk1 (-41.58 kcal mol^{-1}).

The distinction in the shape and nature of the binding site of Plk4 is reflected in the position and orientation of docked CAP-53194. This difference is induced due to the replacement of two crucial residues, Phe183 and Arg136 present in Plk1, required for proper positioning and stabilization of CAP-53194, by Leu142 and Gly95 in Plk4. These substitutions result in the disruption of π–π interactions and cation–π interactions important for stabilization of CAP-53194 aromatic R2 and R1 moieties in Plk1-3. This necessitates the reversal of binding orientation of compound CAP-53194 with respect to its orientation in Plk1-3 in a manner identical to that observed for BI2536 (Fig. 4d). The R1 moiety protrudes towards the surface of the binding pocket while R3 moiety along with the amide linker migrates towards the inner side of the pocket. The nitro groups of R1 and R3 moieties are engaged in hydrogen bonded interactions with Arg28 and Lys41 and their phenyl ring exhibit van der Waals interactions with Leu18 and Val26, respectively as compared to stronger π–π interactions observed between aromatic ring of R1 moiety and Phe183 of Plk1. As a consequence the binding affinity for Plk4 is reduced by approximately 190-fold in comparison to Plk1. This is also reflected by a lesser negative total interaction energy for Plk4 (-42.62 kcal mol^{-1}) as compared to Plk1 (-71.56 kcal mol^{-1}).

We also performed docking studies with other important kinases involved in the cell cycle to assess the selectivity of compound CAP-53194. All the kinases included in this study have a Leu/Met residue (similar to Plk4) instead of Phe183 in Plk1. This leads to loss of crucial aromatic interactions essential for the positioning and stabilization of aromatic R1 moiety of CAP-53194. Similarly, the mutation of residue Arg136, responsible for stabilization of the R2 moiety through cation–π and hydrogen bonded interactions in Plk1, by Gly results in a decrease of binding affinity. The docking calculations for CAP-53194 indicated it to be about 400-fold selective for Plk1 over any of the protein kinases (Table 2) making it a highly selective potential inhibitor for Plk1.

3.6. Molecular dynamics simulation of a fully hydrated model of the final docked complex

The effect of solvent on the binding of the potential inhibitor, CAP-53194, was studied by an explicit solvent MD simulation. The temperature, kinetic energy, potential energy and total energy were found to remain steady with little fluctuation throughout the production phase of simulation. The r.m.s. deviation of the complex (protein + ligand) was in the range of 0.46–1.13 Å. The ligand which was allowed to vary during simulation was seen to be fairly stable. There was slight movement in side chains of Arg57, Lys82, Cys133, Arg134, Arg136 and Asp194 in the presence of solvents to optimize the hydrogen bonded interactions. All the hydrogen bonded interactions present before simulation remained intact throughout the simulation. The movement of R1 phenyl ring was accompanied by movement of Phe183 ring to optimize the parallel displaced π–π interactions (Fig. S1). Similarly, the R1 phenyl ring of the ligand and side chain of Arg136 move closer to each other and result in the optimization of cation–π interactions. While the side chain of Glu69 is observed to move away from R3 phenyl ring to minimize the repulsion between the two carboxylate groups. The solvent molecules also form hydrogen bonded interactions with CAP-53194 in the solvated complex. The results indicate that the ligand as a whole moves into a more stable position with a lower docked energy than before MD simulation. The snapshots of the dynamics trajectory at 0, 2, 4, 6, 8 and 10 ns of the production run are shown in Fig. 5.

3.7. ADMET analysis

A compound must possess certain characteristics related to its absorption, distribution, metabolism and excretion (ADME) before it can be an effective drug. The identified compound was subjected to *in silico* ADME and toxicity analysis with the view to further explore its possibility as a drug-like candidate wherein it was scrutinized against a range of toxicological endpoints including

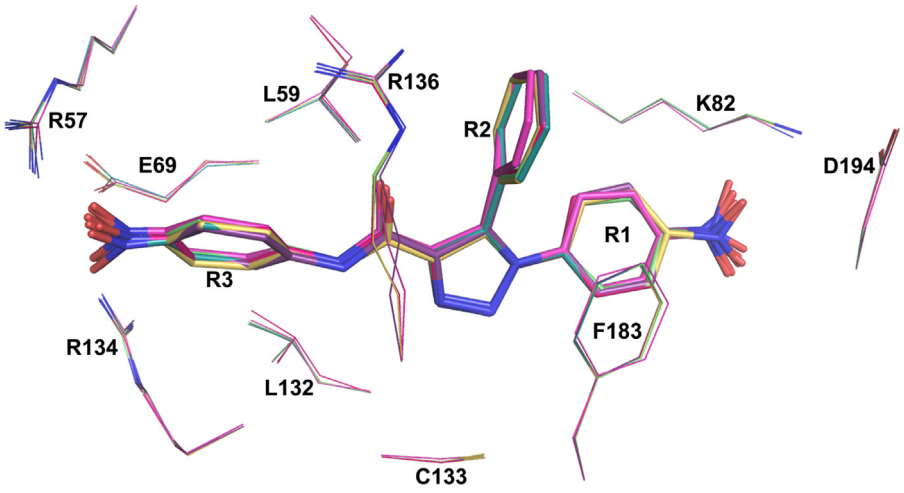

Fig. 5. Molecular dynamics trajectory for the Plk1 complexed with compound CAP-53194. Snapshots of the inhibitor (stick) and selected active site residue conformers (line) extracted from the production dynamics trajectory at the time intervals of 0, 2, 4, 6, 8 and 10 ns.

mutagenicity and carcinogenicity. TOPKAT protocol uses a range of two-dimensional molecular, spatial and electronic descriptors to derive models wherein it applies an Optimal Predictive Space to estimate the reliability of prediction. Any prediction outside this space is taken to be unreliable. CAP-53194 was found to lie within this molecular space. The calculated probability of carcinogenicity of CAP-53194 lies in the lower to intermediate range based on NTP and FDA carcinogenicity and Ames mutagenicity model. It is indicated to have very low probability for developmental toxicity potential. The compound has a molecular weight of 430 Da, a calculated log *P* value of 4.4, 7 hydrogen bond acceptors and 1 hydrogen bond donor indicating that it satisfies the criteria as set by the Lipinski's rule of 5. The polar surface area of 143 $Å^2$ implies that it can cross the cell membrane with good intestinal absorption. The identified compound is thus likely to have good oral bioavailability and the probability of absorption from gut into blood. These parameters suggest that this compound could be a drug-like molecule.

4. Conclusion

Plk1 is an excellent target for discovery of novel anti-mitotic agents for cancer therapy. The high potency inhibitor of Plk1 selective over Plk2 and Plk3 will provide an ideal lead compound for the development of drugs against cancer. The potential inhibitor obtained from virtual screening of LigandFitCAP2002 library showed a differential binding pattern towards Plk family proteins and kinases analysed in this study. The results suggest that this molecule possesses a comparatively higher affinity and greater selectivity towards Plk1 over other Plks and other cell cycle kinases. This is a novel class of Plk1 inhibitor which contains a triazole group and two nitrophenyl moieties. The docking analysis indicates that the identified compound forms a large number of hydrogen bonded interactions with the key residues in the ATP binding pocket of Plk1. This compound in addition to several similar interactions observed with reported Plk inhibitors possesses additional hydrogen bonded interactions formed with Lys82, Arg134, Arg136 and Asp194. The predicted binding constant of CAP-53194 was found to be in the sub-nanomolar range which is more than 10-fold higher when compared to the most potent reported inhibitor of Plk1. The identified potential inhibitor has also been predicted to be about 100-fold selective over other cellular Ser/Thr kinases including the closely related homologues Plk2-4. Since it is predicted to be selective for Plk1, it should exhibit less toxicity than the available lead compounds targeting Plk1. It could, thus, to be taken up further for the development of a novel class of selective molecules against Plk1 for anti-cancer therapy.

Acknowledgements

This project was fully supported by the funds from the Indian Council of Medical Research, New Delhi in the form of the 'Bio-Medical Informatics Centre' Grant No. BIC/9/1/2011.

Appendix A. Supplementary data

Supplementary data associated with this article can be found, in the online version, at http://dx.doi.org/10.1016/j.jmgm.2014.04.014.

References

[1] K. Strebhardt, A. Ullrich, Targeting polo-like kinase 1 for cancer therapy, Nat. Rev. Cancer 6 (2006) 321–330.
[2] U. Holtrich, G. Wolf, A. Brauninger, T. Karn, B. Bohme, H. Rubsamen-Waigmann, K. Strebhardt, Induction and down-regulation of PLK, a human serine/threonine kinase expressed in proliferating cells and tumors, Proc. Natl. Acad. Sci. U.S.A. 91 (1994) 1736–1740.
[3] N. Takai, R. Hamanaka, J. Yoshimatsu, I. Miyakawa, Polo-like kinases (Plks) and cancer, Oncogene 24 (2005) 287–291.
[4] G. Wolf, R. Elez, A. Doermer, U. Holtrich, H. Ackermann, H.J. Stutte, H.M. Altmannsberger, H. Rübsamen-Waigmann, K. Strebhardt, Prognostic significance of polo-like kinase (PLK) expression in non-small cell lung cancer, Oncogene 14 (1997) 543–549.
[5] R. Knecht, R. Elez, M. Oechler, C. Solbach, C. von Ilberg, K. Strebhardt, Prognostic significance of polo-like kinase (PLK) expression in squamous cell carcinomas of the head and neck, Cancer Res. 59 (1999) 2794–2797.
[6] B. Spankuch-Schmitt, G. Wolf, C. Solbach, S. Loibl, R. Knecht, M. Stegmuller, G. von Minckwitz, M. Kaufmann, K. Strebhardt, Downregulation of human polo-like kinase activity by antisense oligonucleotides induces growth inhibition in cancer cells, Oncogene 21 (2002) 3162–3171.
[7] R. Elez, A. Piiper, B. Kronenberger, M. Kock, M. Brendel, E. Hermann, U. Pliquett, E. Neumann, S. Zeuzem, Tumor regression by combination antisense therapy against Plk1 and Bcl-2, Oncogene 22 (2003) 69–80.
[8] X. Liu, R.L. Erikson, Polo-like kinase (Plk)1 depletion induces apoptosis in cancer cells, Proc. Natl. Acad. Sci. U.S.A. 100 (2003) 5789–5794.
[9] J.A. Winkles, G.F. Alberts, Differential regulation of polo-like kinase 1, 2, 3, and 4 gene expression in mammalian cells and tissues, Oncogene 24 (2005) 260–266.
[10] X. Liu, R.L. Erikson, Polo like kinase 1 in the life and death of cancer cells, Cell Cycle 2 (2003) 424–425.
[11] J. Yuan, F. Eckerdt, J. Bereiter-Hahn, E. Kurunci-Csacsko, M. Kaufmann, K. Strebhardt, Cooperative phosphorylation including the activity of polo-like kinase 1 regulates the subcellular localization of cyclin B1, Oncogene 21 (2002) 8282–8292.
[12] F. Eckerdt, K. Strebhardt, Polo-like kinase 1: target and regulator of anaphase-promoting complex/cyclosome-dependent proteolysis, Cancer Res. 66 (2006) 6895–6898.

[13] P. Descombes, E.A. Nigg, The polo-like kinase Plx1 is required for M phase exit and destruction of mitotic regulators in Xenopus egg extracts, EMBO J. 17 (1998) 1328–1335.
[14] Y. Shimizu-Yoshida, K. Sugiyama, T. Rogounovitch, A. Ohtsuru, H. Namba, V. Saenko, S. Yamashita, Radiation-inducible hSNK gene is transcriptionally regulated by p53 binding homology element in human thyroid cells, Biochem. Biophys. Res. Commun. 289 (2001) 491–498.
[15] W.C. Zimmerman, R.L. Erikson, Polo-like kinase 3 is required for entry into S phase, Proc. Natl. Acad. Sci. U.S.A. 104 (2007) 1847–1852.
[16] Y. Yang, J. Bai, R. Shen, S.A. Brown, E. Komissarova, Y. Huang, N. Jiang, G.F. Alberts, M. Costa, L. Lu, J.A. Winkles, W. Dai, Polo-like kinase 3 functions as a tumor suppressor and is a negative regulator of hypoxia-inducible factor-1 alpha under hypoxic conditions, Cancer Res. 68 (2008) 4077–4085.
[17] R. Habedanck, Y.D. Stierhof, C.J. Wilkinson, E.A. Nigg, The Polo kinase Plk4 functions in centriole duplication, Nat. Cell Biol. 7 (2005) 1140–1146.
[18] G. de Carcer, B. Escobar, A.M. Higuero, L. Garcia, A. Anson, G. Perez, M. Mollejo, G. Manning, B. Melendez, J. Abad-Rodriguez, M. Malumbres, Plk5, a polo box domain-only protein with specific roles in neuron differentiation and glioblastoma suppression, Mol. Cell. Biol. 31 (2011) 1225–1239.
[19] D.M. Lowery, D. Lim, M.B. Yaffe, Structure and function of Polo-like kinases, Oncogene 24 (2005) 248–259.
[20] Y. Liu, K.R. Shreder, W. Gai, S. Corral, D.K. Ferris, J.S. Rosenblum, Wortmannin, a widely used phosphoinositide 3-kinase inhibitor, also potently inhibits mammalian polo-like kinase, Chem. Biol. 12 (2005) 99–107.
[21] C.S. Stevenson, E.A. Capper, A.K. Roshak, B. Marquez, C. Eichman, J.R. Jackson, M. Mattern, W.H. Gerwick, R.S. Jacobs, L.A. Marshall, The identification and characterization of the marine natural product scytonemin as a novel antiproliferative pharmacophore, J. Pharmacol. Exp. Ther. 303 (2002) 858–866.
[22] T.J. Lansing, R.T. McConnell, D.R. Duckett, G.M. Spehar, V.B. Knick, D.F. Hassler, N. Noro, M. Furuta, K.A. Emmitte, T.M. Gilmer, R.A. Mook Jr., M. Cheung, *In vitro* biological activity of a novel small-molecule inhibitor of polo-like kinase 1, Mol. Cancer Ther. 6 (2007) 450–459.
[23] A. Santamaria, R. Neef, U. Eberspächer, K. Eis, M. Husemann, D. Mumberg, S. Prechtl, V. Schulze, G. Siemeister, L. Wortmann, F.A. Barr, E.A. Nigg, Use of the novel Plk1 inhibitor ZK-thiazolidinone to elucidate functions of Plk1 in early and late stages of mitosis, Mol. Biol. Cell 18 (2007) 4024–4036.
[24] M. Steegmaier, M. Hoffmann, A. Baum, P. Lénárt, M. Petronczki, M. Krssák, U. Gürtler, P. Garin-Chesa, S. Lieb, J. Quant, M. Grauert, G.R. Adolf, N. Kraut, J.M. Peters, W.J. Rettig, BI2536, a potent and selective inhibitor of polo-like kinase 1, inhibits tumor growth *in vivo*, Curr. Biol. 17 (2007) 316–322.
[25] M. Kothe, D. Kohls, S. Low, R. Coli, G.R. Rennie, F. Feru, C. Kuhn, Y.H. Ding, Selectivity-determining residues in Plk1, Chem. Biol. Drug Des. 70 (2007) 540–546.
[26] H.M. Berman, J. Westbrook, Z. Feng, G. Gilliland, T.N. Bhat, H. Weissig, I.N. Shindyalov, P.E. Bourne, The Protein Data Bank, Nucleic Acids Res. 28 (2000) 235–242.
[27] Discovery Studio, Version 2.0, Accelrys, Inc., San Diego, CA, USA, 2007.
[28] B.R. Brooks, R.E. Bruccoleri, B.D. Olafson, D.J. States, S. Swaminathan, M. Karplus, CHARMM: a program for macromolecular energy, minimization, and dynamics calculations, J. Comput. Chem. 4 (1983) 187–217.
[29] F.A. Momany, R. Rone, Validation of the general purpose QUANTA®3.2/CHARMm® force field, J. Comput. Chem. 13 (1992) 888–900.
[30] C.M. Venkatachalam, X. Jiang, T. Oldfield, M. Waldman, LigandFit: a novel method for the shape-directed rapid docking of ligands to protein active sites, J. Mol. Graph. Model. 21 (2003) 289–307.
[31] A. Sali, T.L. Blundell, Comparative protein modeling by satisfaction of spatial restraints, J. Mol. Biol. 234 (1993) 779–815.
[32] A. Sali, A. Pottertone, F. Yuan, H. van Vlijmen, M. Karplus, Evaluation of comparative protein modeling by MODELLER, Proteins 23 (1995) 318–326.
[33] M.Y. Shen, A. Sali, Statistical potential for assessment and prediction of protein structures, Protein Sci. 15 (2006) 2507–2524.
[34] R.A. Laskowski, M.W. MacArthur, D.S. Moss, J.M. Thornton, PROCHECK: a program to check the steriochemical quality of protein structures, J. Appl. Crystallogr. 26 (1993) 283–291.
[35] S.L. Mayo, B.D. Olafson, W.A. Goddard, DREIDING: a generic force field for molecular simulations, J. Phys. Chem. 94 (1990) 8897–8909.
[36] LigandFit/CAP, Version 1.0, Accelrys, Inc., San Diego, CA, USA, 2006.
[37] C.A. Lipinski, Drug-like properties and the causes of poor solubility and poor permeability, J. Pharmacol. Toxicol. Methods 44 (2001) 235–249.
[38] C.A. Lipinski, F. Lombardo, B.W. Dominy, P.J. Feeney, Experimental and computational approaches to estimate solubility and permeability in drug discovery and development setting, Adv. Drug Deliv. Rev. 46 (2001) 3–26.
[39] J. Sadowski, J. Gasteiger, From atoms and bonds to three-dimensional atomic coordinates: automatic model builders, Chem. Rev. 93 (1993) 2567–2581.
[40] J. Sadowski, J. Gasteiger, G. Klebe, Comparison of automatic three-dimensional model builders using 639 X-ray structures, J. Chem. Inf. Comput. Sci. 34 (1994) 1000–1008.
[41] W.L. Jorgensen, J. Chandrasekhar, J.D. Madura, R.W. Impey, M.L. Klein, Comparison of simple potential functions for simulating liquid water, J. Chem. Phys. 79 (1983) 926–935.
[42] H.J.C. Berendsen, J.P.M. Postma, W.F. van Gunsteren, A. DiNola, J.R. Haak, Molecular dynamics with coupling to an external bath, J. Chem. Phys. 81 (1984) 3684–3690.
[43] H.J. Böhm, Prediction of binding constants of protein ligands: a fast method for the prioritization of hits obtained from de novo design or 3D database search programs, J. Comput. Aided Mater. Des. 12 (1998) 309–323.
[44] M. Vieth, J.D. Hirst, A. Kolinski, C.L. Brooks III, Assessing energy functions for flexible docking, J. Comput. Chem. 19 (1998) 1612–1622.
[45] The PyMOL Molecular Graphics System, Version 0.99rc6, DeLano Scientific, San Carlos, CA, USA, 2006.